Priority-Aware Layered Offloading in Cooperative UAV-MEC Networks via SPC-NOMA

Anfal R. Desher * and Ali Al-Shuwaili

Posted Date: 31 March 2026

doi: 10.20944/preprints202603.2442.v1

Keywords: cooperative UAVs; UAV trajectory; layered transmission (LT); non-orthogonal multiple access (NOMA); superposition coding (SPC); multi-access edge computing (MEC)

 doi:10.20944/preprints202603.2442.v1

Article

Priority-Aware Layered Offloading in Cooperative UAV-MEC Networks via SPC-NOMA

Anfal R. Desher [1,*] and Ali Al-Shuwaili [2]

[1] Mobile Communications and Computing Engineering, University of Information Technology and Communications, Baghdad 10001, Iraq

[2] College of Engineering, University of Information Technology and Communications, Baghdad 10001, Iraq

* Correspondence: anfal.raad.gs@uoitc.edu.iq

Abstract

UAV-based Multi-Access Edge Computing (MEC) systems are vital solutions in disaster scenarios by providing temporary radio and processing resources to rescue teams and survivors. However, recent schemes in the literature typically treat offloaded tasks as one indivisible units and fail to account for heterogeneous reliability requirements, leading to non-optimal resource utilization and performance deterioration under such emergency conditions. Moreover, the joint optimization of communication, computation, and UAV path planning in cooperative setup remains inadequately addressed. This paper proposes a priority-aware layered task offloading framework for cooperative UAV-MEC networks based on Superposition Coding (SPC) and non-orthogonal access. The proposed design separates tasks into reliability-critical base-layer (BL) and enhancement-layer (EL) components, to assure reliable and timely transmission and execution. BL data is prioritized via *intra*- and *inter*-user constraints, while EL data is adaptively processed locally or offloaded via a cooperative UAVs. A joint latency minimization problem is formulated and tackled using an alternating optimization framework with successive convex approximation (AO-SCA). Simulation results demonstrate that the proposed scheme significantly outperforms baseline methods. For 20 users, it achieves a processing efficiency of 92.3%, compared to over 83% for baseline schemes. As the number of users increases to 120, the proposed method maintains superior efficiency at 63.1%, outperforming NC-SPC (40.3%), FT-Coop (51.3%), SL-NOMA (52.4%), and L-OMA (45.3%), highlighting its robustness and scalability in meeting reliability and low-latency requirements in post-disaster scenarios.

Keywords: cooperative UAVs; UAV trajectory; layered transmission (LT); non-orthogonal multiple access (NOMA); superposition coding (SPC); multi-access edge computing (MEC)

1. Introduction

Natural disasters such as earthquakes, floods, and hurricanes cause significant damage to terrestrial communication infrastructure. In such situations, Unmanned Aerial Vehicles (UAVs)-aided communication systems are highly suitable due to their mobility between the nodes [1]. In such scenarios, it is of utmost importance that the requirements are met with ultra-low latency, high reliability, lower energy consumption, and heterogeneous demands of the users [2].

In disaster scenarios such as earthquake relief and flood relief, real-time communication such as victim detection and mapping can be performed using Mobile Edge Computing (MEC), which can be integrated with Unmanned Aerial Vehicles (UAVs), thus minimizing end-to-end delay [3]. In the case of large-scale disaster scenarios, it has been observed that the capabilities of a single UAV might be limited in terms of providing sufficient coverage and computational capabilities. In such scenarios, the role of multi-UAV cooperation becomes crucial in order to enhance the scalability and robustness of the system [4]. The unique advantage of the UAV-assisted system lies in the controllable mobility aspect. It brings in the aspect of trajectory optimization as a new design aspect. It has been observed that the trajectory of the UAV has a direct impact on the channel gain, interference, propulsion energy

 doi:10.20944/preprints202603.2442.v1

consumption, and fairness [5]. With the optimization of the trajectory, the UAV can achieve the highest disparity in the channel gain.

To increase spectral efficiency and accommodate massive connectivity requirements, Non-Orthogonal Multiple Access (NOMA) technology is employed [6],[7]. In NOMA technology, superposition coding is performed at the transmitter and Successive Interference Cancellation (SIC) at the receiver, thus performing power-domain multiplexing and allocating higher power to the users with worse channel conditions to enable reliable communication.

Several existing systems have been designed to execute tasks as a single unit, without taking into consideration the need to prioritize the execution of critical task in a post-disaster scenario.

Our main contributions:

- We propose a comprehensive framework for jointly optimizing UAV trajectory, multi-UAV cooperation, and reliability to prioritize differentiated service requirements. Layered transmission is incorporated into the SPC-NOMA framework (see **Figure 1**). In this scheme, each task is divided into a base layer carrying critical information (e.g., victim location) and an enhancement layer carrying non-essential information. Higher transmission power is allocated to the base layer to ensure reliable reception even under poor channel conditions, subject to strict latency and reliability constraints.
- Scalable Multi-UAV Cooperative Design: A cooperative strategy is developed to improve the scalability of the UAV system in the context of emergency communication networks through UAVs trajectory coordination.

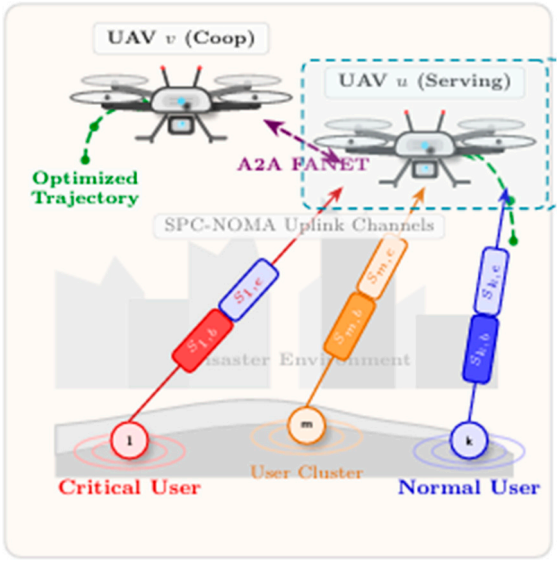

Figure 1. Task's prioritization (Intra-user priority) and user's prioritization (Inter-user priority) in cooperative UAVs via SPC-NOMA framework.

The structure of this paper is as follows. Related works are presented in Section II. In Section III, the channel model, the layered task model, UL communication model, computation model, DL transmission model, and optimization problem formulation are all cleared and discussed. In Section IV, the solution approach is given. After that, the discussion of the obtained results is given in Section V with the aim of showing the effectiveness of the proposed algorithm compared with the several baseline algorithms. Finally, the conclusion of this paper is highlighted in Section VI.

2. Related Works

Many studies focus on UAV-aided MEC with intelligent optimization for enhanced computation offloading. In [8], deep reinforcement learning with the involvement of the UAV as a mobile base

 doi:10.20944/preprints202603.2442.v1

station helps improve the computation offloading process. [9],[10] presents a dual-layer HUAV-LUAV solution for vehicular edge computing to reduce delay and energy costs. The work presented in [8],[9],[10] may be less effective for highly mobile devices.

While studies [11],[12] proposes a wireless powered MEC scheme using a UAV as a means for energy and computing assistance for ground users. The proposed solution is beneficial in terms of energy consumption, but the drawbacks of both models lie in their assumption of equal user demand requirements without focusing on addressing communication priority, non-orthogonal communication techniques, and collaborative communication between UAVs. Also [13] examine energy-efficient UAV-based MEC through the optimization of UAV trajectory, communication resources, and computation load in energy-efficient ways using SCA and Dinkelbach-based optimization methods. Even though there are substantial improvements in energy efficiency, there is homogeneous demand treated and nothing related to latency-sensitive and priority-aware services.

Ref. [14] deals with the multi-UAV system of the MEC and uses reinforcement learning to address the user association and resource allocation tasks simultaneously. In this case, the reinforcement learning method improves scalability and adaptability. However, the method treats the users equally without making a distinction between the critical and the non-critical services. Meanwhile, [15] describe a UAV supported MEC system in which mobile users compete for common computing resources of the UAV modeled by a stochastic game to be solved by proactive DRL with LSTM. Although it is helpful in optimizing long-term system performances, it fails to accomplish priority distinction in services of users and emergency-driven quality-of-service. [16] presented a framework for computation offloading using Mobile Edge Computing (MEC), along with the demonstration of the reduction in the total offloading latency using decoupled uplink and downlink base station association, despite the additional latency due to the backhaul delay, the problem of trade-off between reliability and latency is not completely addressed.

There are many works are significant to the topic of FANETs. [17] presents a classification of FANET applications and proves that general random mobility patterns are not accurate for UAVs. [18] gives a survey of architectures of FANETs, as well as mobility and security aspects. It also points out that there are no unified and secure solutions for FANETs.

While [19] the trajectory generation module of the SPASAS system, which utilizes MILP and a modified version of the A* algorithm, is presented, used for optimal path planning of UAVs in static and dynamic scenarios with pop-up threats, with real-time re-optimization and radar risk minimization; however, the paper mainly deals with the case of single UAV operation, assumes known models of threat probabilities, and has limited integration of onboard sensing.

Current researches on UAV-assisted networks shed light on the efficient communication and computation for the FANET and MEC supported systems. [20] presents the concept of a multi-layered UAV network implemented with the hybrid IEEE 802.11/802.15.1 model targeting the sum of throughput, delay, and energy consumed. Even though the research provides insights into the energy-efficient strategy for UAV-assisted networks, focusing only on the reliable communication process without considering the optimization process, still [21] provides an idea of the distributed UAV-assisted MEC system for the 5G networks implemented with the fuzzy-logic link assessment process and the multi-agent deep reinforcement learning technique.

Moreover, [22] suggests that the mobility of UAVs, together with edge computing, can provide flexible and latency-capable services in an infrastructure-deprived network. However, many technical difficulties still need to be overcame in order to successfully deploy such solutions on a large scale in the future, such as the UAVs' energy, communication, security, priority, and real-time computing requirements. While [23], presents the development of an empirical model of LoS probability depending on altitude in air-to-ground communications via LoS / NLoS classification using KNN-based techniques in combination with neural networks for estimating model parameters. This empirical model matches well with ray-tracing simulation, measurement campaigns, and traditional models while allowing a broad range of altitudes for UAV, without focusing on addressing communication priority and non-orthogonal communication techniques.

 doi:10.20944/preprints202603.2442.v1

Ref. [24] suggests a reliable access scheme using ML for a UAV network, which uses K-means clustering to cluster users and apply NOMA or OMA, and optimizes the altitude and power allocation of the UAV to achieve maximum coverage under reliability constraints, but it assumes correct channel information and uses simulation, which might not be practical in a dynamic environment. While [25] introduces a strategy for improving robustness in drone fleet communication by using fault tree analysis to analyze communication risks and implementing a protocol that uses retransmission with a minimum of 11 attempts to ensure 99% reliability of data delivery from drones to the Ground Station Control, although this strategy results in increased communication overhead and latency and is primarily tested analytically rather than through comprehensive real-world testing.

Also [26] presents a machine learning-based reliability classification framework for mission reliability evaluation, coverage reliability evaluation, and link quality evaluation for UAV inspection missions in power and energy systems based on gradient boosting machine learning algorithms; however, it utilizes artificial data sets and has class imbalance problems.

While a lot of work has been done (see **Table 1**) in the areas of UAV communication, NOMA, MEC, and trajectory optimization individually, a unified framework for joint optimization of SPC-NOMA transmission, layered priority communication, UAV-enabled MEC, trajectory optimization, and multi-UAV cooperation in disaster scenarios is not adequately explored. These areas need to be considered in a holistic manner to unlock the potential offered by UAVs in emergency communication scenarios and satisfy the stringent quality-of-service constraints of future disaster response networks.

This research aims to examine the issue of priority-aware task offloading and communication-computation resource optimization in cooperative UAVs-assisted MEC via SPC-NOMA technology.

The questions to be answered in this research include:

- How to incorporate the issue of task prioritization via SPC-NOMA technology in cooperative FANET architectures to ensure differentiated QoS for critical missions?
- How to jointly optimize communication and computation resources of cooperative UAVs to minimize E2E (End-to-End) latency in resource-constrained networks?

Table 1. Comparison of this paper with related works.

Reference	UAV	MEC	Priority	NOMA	SPC	Trajectory
[28]	✓			✓	✓	
[29]	✓	✓		✓	✓	
[30]	✓			✓	✓	✓
[31]	✓	✓		✓	✓	✓
[32]	✓	✓		✓	✓	✓
[33]	✓	✓		✓	✓	
[34]	✓					✓
[35]	✓			✓	✓	✓
[36]	✓			✓	✓	✓
[37]	✓			✓	✓	
[38]	✓	✓				✓
This paper	✓	✓	✓	✓	✓	✓

3. System Model

We consider a UAV-assisted multi-access edge computing (MEC) system consisting of:

- Aset of ground users $\boldsymbol{i} = \{\mathbf{1}, \mathbf{2}, \mathbf{3}, \ldots \mathbf{I}\}$.
- Aset of UAV-mounted MEC servers $\boldsymbol{u} = \{\mathbf{1}, \mathbf{2}, \mathbf{3}, \ldots \mathbf{U}\}$.
- A cooperative Flying Ad-Hoc Network (FANET) among UAVs.

 doi:10.20944/preprints202603.2442.v1

Time is discretized into N equal-duration slots indexed by $\mathcal{N} = \{1,...,N\}$ with slot length Δt. The overall mission duration is $T \triangleq N\Delta t$.

The horizontal trajectory of UAV u is denoted by:

$$\boldsymbol{q_u[n]} \in \mathbf{R^2}, \forall\, \boldsymbol{n} \in \boldsymbol{\mathcal{N}} \tag{1}$$

And, the trajectory of UAV is constrained by maximum speed V_{max}:

$$\|q_u[n+1] - q_u[n]\| \leq V_{max}\Delta t \tag{2}$$

The initial and final positions are fixed as:

$$q_u[1] = q_u^{ini} \text{ and } q_u[\mathrm{N}] = q_u^F \tag{3}$$

Each UAV flies at fixed altitude H, and each user $\boldsymbol{i}$ is located at fixed position $\boldsymbol{W_i} \in \boldsymbol{R^2}$. Each user is associated with one serving UAV denoted by $u(i)$. So, the distance between the UAV u and user $\boldsymbol{i}$ [27] at slot n is expressed as:

$$\boldsymbol{d_{i,u}[n]} = \sqrt{\left\|\boldsymbol{q_{u(i)}[n]} - \boldsymbol{W_i}\right\|^2 + \boldsymbol{H^2}} \tag{4}$$

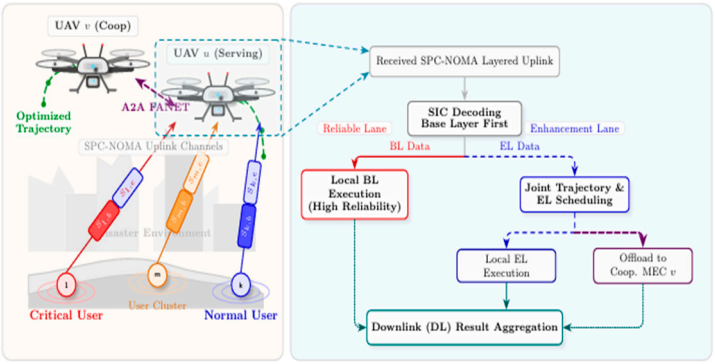

Figure 2. System model of the proposed trajectory-aware UAV-assisted MEC system with power-domain NOMA and superposition coding (SPC). Multiple ground users offload layered computation tasks consisting of reliability-critical base layers and enhancement layers. All users transmit simultaneously via SPC-NOMA in the uplink. Base layers are assigned higher power and decoded first at the UAV using SIC, guaranteeing reliable execution of high-priority tasks. The UAV trajectory $q_u[n]$ is jointly optimized to enhance channel quality and reduce end-to-end latency.

A. *CHANNEL MODEL*

This section describes a channel model for a cooperative flying ad-hoc network (FANET) network. The channel model adheres to ground-to-air (G2A), air-to-air (A2A), and air-to-ground (A2G) communication, in accordance with TR 38.901 standard [39].

(1) GROUND-TO-AIR AND AIR-TO-GROUND CHANNEL MODEL

Both of G2A (uplink) and A2G (downlink) wireless links share similar large-scale propagation properties because of channel reciprocity. The channel power gain between user i and uav $u(i)$ [27] at slot n is:

$$|h_i[n]|^2 = \frac{\beta_0}{\left\|q_{u(i)}[n] - W_i\right\|^2 + H^2} \tag{5}$$

where β_0 is the reference channel gain at 1 meter.

(2) AIR-TO-AIR CHANNEL MODEL

The air-to-air (A2A) channel gain between uav u and uav v is:

$$\left|h_{u,v}[n]\right|^2 = \frac{\beta_0}{\|q_u[n] - q_v[n]\|^2 + H^2} \tag{6}$$

B. *LAYERED TASK MODEL*

 doi:10.20944/preprints202603.2442.v1

Each user i has a layered computation task consisting of a base layer (BL) represented as $S_{i,b}^{UL}$ and measured in bits, and an enhancement layer (EL) represented as $S_{i,e}^{UL}$ and also measured in bits.

Each bit requires iCPU cycles. Also, BL is always executed at the serving UAV, while the EL may be executed locally or forwarded via FANET.

C. *UL COMMUNICATION MODEL*

To ensure effective support for multiple users with limited spectral resources, a power-domain SPC-NOMA scheme is employed in UL transmission. Users transmit their signals simultaneously over the same time-frequency resources.

All users associated with UAV u transmit simultaneously using power-domain NOMA with superposition coding. Let users be ordered such that:

$$|h_1[n]|^2 \geq |h_2[n]|^2 \geq |h_i[n]|^2$$

Each user splits power:

$$P_{i,b}^{UL}[n] + P_{i,e}^{UL}[n] \leq P_i^{max}$$

The received signal at UAV $u(i)$ is:

$$y[n] = \sum_{i \in I_u} h_i[n] \left(\sqrt{P_{i,b}^{UL}[n]} S_{i,b}^{UL}[n] + \sqrt{P_{i,e}^{UL}[n]} S_{i,e}^{UL}[n] \right) + n[n] \quad (7)$$

The potential uplink transmission rates for BL and EL tasks can be calculated as:

$$R_{i,b}[n] = B \log_2 \left(1 + \frac{P_{i,b}^{UL}[n] \, |h_i[n]|^2}{P_{i,e}^{UL}[n] \, |h_i[n]|^2 + \sum_{j>i} |h_j[n]|^2 (P_{j,b}^{UL}[n] + P_{j,e}^{UL}[n]) + N_0} \right) \quad (8)$$

$$R_{i,e}[n] = B \log_2 \left(1 + \frac{P_{i,e}^{UL}[n] \, |h_i[n]|^2}{\sum_{j>i} |h_j[n]|^2 (P_{j,b}^{UL}[n] + P_{j,e}^{UL}[n]) + N_0} \right) \quad (9)$$

Since UAV mobility yields time-varying rates $\{R_{\ell,i}[n]\}_{n=1}^{N}$ for layer $\ell \in \{b, e\}$, we define the accumulated uplink throughput over the mission horizon:

$$R_{i,b}^{UL} \triangleq \sum_{n=1}^{N} \Delta t R_{i,b}[n], \; R_{i,e}^{UL} \triangleq \sum_{n=1}^{N} \Delta t R_{i,e}[n] \quad (10)$$

The corresponding uplink transmission latencies are defined as:

$$\Delta_{i,b}^{UL} \triangleq \frac{S_{i,b}^{UL}}{R_{i,b}^{UL}}, \quad \Delta_{i,e}^{UL} \triangleq \frac{S_{i,e}^{UL}}{R_{i,e}^{UL}} \quad (11)$$

Lemma 1 (Priority-Aware Base-Layer Decodability). Under the proposed SPC–NOMA uplink scheme, if the reliability constraint:

$$R_{i,b}[n] \geq R_{i,b}^{min} \quad (12)$$

is satisfied for all i, n, then the base layer of every user is guaranteed to be decodable at the serving UAV regardless of the enhancement-layer transmission.

Proof. In the SPC transmission model, the received signal at the UAV is:

$$y[n] = \sum_{i} h_i[n] \left(\sqrt{P_{i,b}^{UL}[n]} S_{i,b}^{UL}[n] + \sqrt{P_{i,e}^{UL}[n]} S_{i,e}^{UL}[n] \right) + n[n]$$

The UAV performs successive interference cancellation (SIC) following the decoding order defined by channel strength. When decoding the base layer of user i, the enhancement layer of the same user and the signals of weaker users are treated as interference. Therefore, the achievable base-layer rate is:

$$R_{i,b}[n] = B \log_2 \left(1 + \frac{P_{i,b}^{UL}[n] \, |h_i[n]|^2}{P_{i,e}^{UL}[n] \, |h_i[n]|^2 + I_i[n]} \right)$$

 doi:10.20944/preprints202603.2442.v1

If $R_{i,b}[n] \geq R_{i,b}^{min}$ holds, the SINR of the base layer is sufficient to support the target coding rate. Hence the base layer can always be decoded successfully before enhancement layer decoding.

D. ***COMPUTATION MODEL***

Each UAV u has total CPU capacity F_u^{max}. The computation latency is defined according to the allocated CPU resources for both BL and EL. The BL computation latency:

$$\Delta_{i,b}^{MEC} = \frac{i\, S_{i,b}^{UL}}{f_{i,b}^{MEC}} \tag{13}$$

while, the EL computation latency:

$$\Delta_{i,e}^{MEC} = (1-\xi)\,\frac{i\, S_{i,e}^{UL}}{f_{i,e}^{MEC}} + \xi\,\frac{i\, S_{i,e}^{UL}}{f_{i,e}^{MEC}} \tag{14}$$

where ξ refer to the execution indicator (for EL only) and equal to:

$$\xi_i = \begin{cases} 1, if\ the\ \text{EL of user } i \text{ is executed via FANET cooperation,} \\ 0, if\ the\ \text{EL of user } i \text{ is executed locally at the serving UAV.} \end{cases}$$

If $\xi_i = 1$, EL is forwarded to UAV v. The A2A rate:

$$R_{u\leftrightarrow v}^{A2A}[n] = B_{A2A}\, log_2\left(1 + \frac{P_u^{A2A}[n]\,\left|h_{u,v}[n]\right|^2}{N_0}\right) \tag{15}$$

Define the accumulated A2A throughput and its latency surrogate:

$$, \quad \Delta_{i,e}^{A2A} \triangleq \xi_i \frac{S_{i,e}^{UL}}{R_i^{A2A}} \quad (16)$$

$$R_i^{A2A} \triangleq \sum_{n=1}^{N} \Delta t R_{u\leftrightarrow v}^{A2A}[n] \tag{16}$$

The current model includes local CPU constraints, but the cooperative UAV that receives forwarded EL tasks must also satisfy its own computational capacity limit:

$$\sum_{i\epsilon I_v^{loc}} \left(f_{i,b}^{MEC} + (1-\xi_i) f_{i,e}^{MEC,(v)}\right) + \sum_{i\epsilon I_v^{coop}} (\xi_i) f_{i,e}^{MEC,(v)} + \leq F_u^{max} \ , \qquad \forall\, v \in U \tag{17}$$

Lemma 2 (Optimal CPU Allocation). For a given UAV u, the optimal CPU allocation minimizing the weighted computation latency:

$$\sum_{i\epsilon I_u} W_i \frac{i\, S_{i,b}^{UL}}{f_{i,b}^{MEC}}$$

subject to

$$\sum_{i\epsilon I_u} f_{i,b}^{MEC} \leq F_u^{max}$$

is given by

$$f_{i,b}^{MEC\,*} = F_u^{max} \sqrt{\left(w_i\, S_{i,b}^{UL}\right)} / \sum_{j\,\in\, I_u}^{\mathrm{I}} \sqrt{\left(w_j S_{j,b}^{UL}\right)} \tag{18}$$

Proof. The problem is convex since $1/f$ is convex for $f > 0$. The Lagrangian is:

$$L = \sum_i W_i \frac{i\, S_{i,b}^{UL}}{f_{i,b}^{MEC}} + \lambda\left(\sum_i f_{i,b}^{MEC} \leq F_u^{max}\right)$$

Taking derivatives and setting them to zero gives:

 doi:10.20944/preprints202603.2442.v1

$$-w_i \frac{i\, S_{i,b}^{UL}}{f_{i,b}^{MEC2}} + \lambda =$$

Solving for $f_{i,b}^{MEC}$ yields:

$$f_{i,b}^{MEC} = \sqrt{w_i \frac{i\, S_{i,b}^{UL}}{\lambda}}$$

Using the total CPU constraint determines λ and yields the closed-form solution above.

E. *DL TRANSMISSION MODEL*

In the downlink, orthogonal multiple access (OMA) is adopted. Let $P_{i,u}^{DL}[n]$ denote the downlink transmit power allocated by UAV $u(i)$ to user i at slot n. The downlink rate of user i at slot n is modeled as:

$$R_i^{DL}[n] = B_{DL}\, log_2\left(1 + \frac{P_{i,u(i)}^{DL}[n]\, |h_i[n]|^2}{N_0}\right) \quad (19)$$

Define accumulated DL throughput and latency surrogates:

$$R_{i,b}^{DL} \triangleq \sum_{n=1}^{N} \Delta t R_i^{DL}[n], \quad R_{i,e}^{DL} \triangleq \sum_{n=1}^{N} \Delta t R_i^{DL}[n] \quad (20)$$

$$\Delta_{i,b}^{DL} \triangleq \frac{S_{i,b}^{DL}}{R_{i,b}^{DL}}, \quad \Delta_{i,e}^{DL} \triangleq \frac{S_{i,e}^{DL}}{R_{i,e}^{DL}} \quad (21)$$

F. *END-TO-END LATENCY*

The BL latency is equal to:

$$\Delta_{i,b} = \Delta_{i,b}^{UL} + \Delta_{i,b}^{MEC} + \Delta_{i,b}^{DL} \quad (22)$$

Meanwhile, the EL latency is equal to:

$$\Delta_{i,e} = \Delta_{i,e}^{UL} + \Delta_{i,e}^{A2A} + \Delta_{i,e}^{MEC} + \Delta_{i,e}^{DL} \quad (23)$$

So, the End-to-End (E2E) latency can be calculated as:

$$\Delta_i^{E2E} = \Delta_{i,b} + \Delta_{i,e} \quad (24)$$

G. *PROBLEM FORMULATION*

The aim of this section is to optimize the allocation of communication and computing resources jointly so, that E2E latency is reduced for critical users in latency-sensitive mission applications under cooperative UAV FANET that enables MEC technology, which is formulated mathematically as in $\boldsymbol{P.1}$:

$$\min_{\left(P_{i,b}^{UL}, P_{i,e}^{UL}, f_{i,b}^{MEC}, f_{i,e}^{MEC}, P_{i,u}^{DL}, \xi, q\right)} \sum_{i=1}^{I} w_i\, \Delta_i^{E2E} \quad (\boldsymbol{P.1})$$

S.t:

(C.1) $\boldsymbol{R_{i,b}[n] \geq R_{i,b}^{min}}$, $\forall\, \boldsymbol{i}, \forall\, \boldsymbol{n}$

(C.2) $\boldsymbol{P_{i,b}^{UL}[n] > P_{i,e}^{UL}[n]}$, $\forall\, \boldsymbol{i, n}$

(C.3) $\sum_{i:\, \xi_i = 1} \boldsymbol{f_{i,e}^{MEC,(v)} \leq F_v^{max}}$

(C.4) $\sum_{i \epsilon u}^{I} \boldsymbol{P_{i,u}^{DL}[n] \leq P_u^{max}}$, $\forall\, \boldsymbol{i, n}$

(C.5) $\sum_{i \epsilon I_u} \left(\boldsymbol{f_{i,b}^{MEC} + (1 - \xi_i) f_{i,e}^{MEC,u}}\right) \leq \boldsymbol{F_u^{max}}$, $\forall\, \boldsymbol{u}$

(C.6) $\boldsymbol{\xi \in \{0, 1\}}$, $\forall\, \boldsymbol{u}$

(C.7) $\sum_{n=1}^{N} \boldsymbol{\Delta t R_{i,b}[n] \geq S_{i,b}^{UL}}$, $\sum_{n=1}^{N} \boldsymbol{\Delta t R_{i,e}[n] \geq S_{i,e}^{UL}}, \forall\, \boldsymbol{i}$

(C.8) $\boldsymbol{\Delta_i^{E2E} \leq \Delta_i^{max}}$, $\forall\, \boldsymbol{i}$

(C.9) $\boldsymbol{P_{i,b}^{UL}[n], P_{i,e}^{UL}[n], f_{i,b}^{MEC}, f_{i,e}^{MEC}, P_{i,u}^{DL}[n] \geq 0}$, $\forall\, \boldsymbol{i}$

(C.10) $\boldsymbol{R_i^{A2A} \geq \xi_i S_{i,e}^{UL}}$, $\forall\, \boldsymbol{i}$

(C.11) $\sum_{n=1}^{N} \boldsymbol{\Delta t R_i^{DL}[n] \geq S_{i,b}^{DL}}$, $\sum_{n=1}^{N} \boldsymbol{\Delta t R_i^{DL}[n] \geq S_{i,e}^{DL}}$, $\forall\, \boldsymbol{i}$

(C.12) $\sum_{n=1}^{N} \boldsymbol{\Delta t R_{u \leftrightarrow v}^{A2A}[n] \geq \xi_i S_{i,e}^{UL}}, \forall\, \boldsymbol{i}$

 doi:10.20944/preprints202603.2442.v1

($\boldsymbol{P.1}$) indicates that there are three kinds of priority: one is the user-level priority according to user weights where higher w_i assigned to critical users, the second is the layer-level priority as clear in (C.1), and the other is network-level priority when BL executed locally and only EL may use FANET.

Constraints (C.1) guarantees reliable BL decoding for each user; (C.2) refers to the power allocated for BL is always greater than power allocated for EL for each user; (C.3) indicates the CPU constraints for cooperative UAV v; (C.4) emphasizes that the UAV power for $i-th$ users beloinging to UAV u is smaller than or equal to the maximum UAV power; (C.5) This constraint takes into account the finite computational capability for each UAV. It is ensured that the computation for all users' BL is always guaranteed, and the computation for users' EL is determined by the activation variable ($\boldsymbol{\xi}$), thus enabling the handling of UAV overload situations; (C.6) introduces a binary decision variable that dictates the execution of EL tasks on a given UAV, which promotes flexibility in executing EL tasks or offloading/deferring EL tasks in response to variations in load on UAV; (C.7) enforces the throughput feasibility constraints to ensure deliverability within the mission horizon; (C.8) assures that the E2E delay of each critical user remains less than its maximum tolerable E2E delay. This constraint directly reflects the critical quality of service (QoS) requirements of disaster-response, emergency services; (C.9) non-negativity constraint guarantees the physical feasibility of all the allocation variables for the resources of power and computation for each user; (C.10) enforces feasibility (only when $\xi_i = 1$); (C.11) enforce deliverability constraints of DL task; and (C.12) ensures that required bits is actually delivered within the mission horizon.

4. Solution Approach

A. *PROBLEM ANALYSIS*

- Nonconvex UL SPC–NOMA rates

The BL achievable rate of user i in slot n can be written as:

$$R_{i,b}[n] = Blog_2\left(|h_i[n]|^2\left(P_{i,b}^{UL}[n] + P_{i,e}^{UL}[n]\right) + I_i[n]\right) - Blog_2\left(|h_i[n]|^2 P_{i,e}^{UL}[n] + I_i[n]\right), \quad (25)$$

where:

$$I_i[n] = \sum_{j>i} \left|h_j[n]\right|^2\left(P_{j,b}^{UL}[n] + P_{j,e}^{UL}[n]\right) + N_0$$

This expression is the difference of two concave functions and therefore nonconcave in the transmit power variables.

- Trajectory–channel coupling

The channel gain depends on the UAV position as:

$$|\boldsymbol{h_i}[\boldsymbol{n}]|^2 = \boldsymbol{\beta_0}/\left(\left|\left|\boldsymbol{q_{u(i)}}[\boldsymbol{n}] - \boldsymbol{W_i}\right|\right|^2 + \boldsymbol{H^2}\right),$$

which leads to a nonconvex dependence of the achievable rates on the UAV trajectory.

- Binary FANET decision

The enhancement-layer execution indicator $\xi_i \in 0,1$ introduces integer variables.

Therefore, problem $\boldsymbol{P.1}$ is a mixed-integer nonconvex program. We develop an alternating optimization (AO) framework combined with successive convex approximation (SCA).

B. *LATENCY REPRESENTATION*

Define accumulated throughputs over the mission horizon $T = N\Delta t$:

$$R_{i,b}^{UL} = \sum_{n=1}^{N} \Delta t R_{i,b}[n] \quad (26)$$

$$R_{i,e}^{UL} = \sum_{n=1}^{N} \Delta t R_{i,e}[n] \quad (27)$$

$$R_i^{DL} = \sum_{n=1}^{N} \Delta t R_i^{DL}[n] \quad (28)$$

 doi:10.20944/preprints202603.2442.v1

$$R_i^{A2A} = \sum_{n=1}^{N} \Delta t R_{u\leftrightarrow v}^{A2A}[n] \tag{29}$$

The uplink, downlink, and FANET transmission latencies are expressed as:

$$\Delta_{i,b}^{UL} = \frac{S_{i,b}^{UL}}{R_{i,b}^{UL}} \tag{30}$$

$$\Delta_{i,e}^{UL} = \frac{S_{i,e}^{UL}}{R_{i,e}^{UL}} \tag{31}$$

$$\Delta_{i,b}^{DL} = \frac{S_{i,b}^{DL}}{R_{i,b}^{DL}} \tag{32}$$

$$\Delta_{i,e}^{DL} = \frac{S_{i,e}^{DL}}{R_{i,e}^{DL}} \tag{33}$$

$$\Delta_{i,e}^{A2A} = \frac{S_{i,e}^{UL}}{R_i^{A2A}} \tag{34}$$

To guarantee that all tasks are completed within the mission horizon, the following deliverability constraints are imposed:

$$R_{i,b}^{UL} \geq S_{i,b}^{UL} \tag{35}$$

$$R_{i,e}^{UL} \geq S_{i,e}^{UL} \tag{36}$$

$$R_i^{DL} \geq S_{i,b}^{DL} + S_{i,e}^{DL} \tag{37}$$

$$R_i^{A2A} \geq \xi_i S_{i,e}^{UL} \tag{38}$$

C. *ALTERNATING OPTIMIZATION FRAMEWORK*

The optimization variables are grouped into the following blocks:

- UAV trajectory $q_u[n]$
- UL transmit powers $P_{i,b}^{UL}[n], P_{i,e}^{UL}[n]$
- DL transmit powers $P_{i,u}^{DL}[n]$
- CPU allocation $f_{i,b}^{MEC}$, $f_{i,e}^{MEC}$
- FANET decisions ξ_i

We optimize these blocks iteratively using alternating optimization. At each iteration, one block is optimized while the remaining variables are fixed.

D. *CLOSED-FORM CPU ALLOCATION*

For fixed communication variables and offloading decisions, the BL computation latency minimization becomes:

$$\min_{f_{i,b}^{MEC}} \sum_{i \in I_u}^{\mathrm{I}} w_i \frac{i\, S_{i,b}^{UL}}{f_{i,b}^{MEC}} \quad \text{s.t. } \sum_{i \in I_u}^{\mathrm{I}} f_{i,b}^{MEC} \leq F_u^{max} \tag{39}$$

This problem is convex. Applying the KKT conditions yields the optimal CPU allocation

$$f_{i,b}^{MEC\,*} = F_u^{max} \sqrt{\left(w_i S_{i,b}^{UL}\right)} / \sum_{j \in I_u}^{\mathrm{I}} \sqrt{\left(w_j S_{j,b}^{UL}\right)} \tag{40}$$

The same structure applies to enhancement-layer computation by replacing $\boldsymbol{S_{i,b}^{UL}}$ with $\boldsymbol{S_{i,e}^{UL}}$.

E. *UL POWER OPTIMIZATION VIA SPC*

For fixed trajectory and CPU allocation, the UL power allocation remains nonconvex due to the NOMA rate structure. The BL rate can be expressed as:

$$R_{i,b}^{UL}[n] = g_1(P) - g_2(P)$$

 doi:10.20944/preprints202603.2442.v1

where both g_1 and g_2 are concave functions. The second term is linearized using first order Taylor approximation at the current iterate, which yields a concave lower bound of the rate. The resulting power subproblem becomes convex and can be efficiently solved. For completeness, we explicitly show the surrogate construction used in the proposed AO–SCA algorithm.

(1) SCA FOR THE UL BL RATE

Recall that the bl achievable rate is:

$$R_{i,b}[n] = Blog_2\left(|h_i[n]|^2\left(P_{i,b}^{UL}[n] + P_{i,e}^{UL}[n]\right) + I_i[n]\right) - Blog_2\left(|h_i[n]|^2 P_{i,e}^{UL}[n] + I_i[n]\right), \quad (41)$$

where:

$$I_i[n] = \sum\nolimits_{j>i} \left|h_j[n]\right|^2\left(P_{j,b}^{UL}[n] + P_{j,e}^{UL}[n]\right) + N_0$$

The first term is concave in the power variables, while the second term is also concave but appears with a negative sign. Hence, (41) has a standard dc structure.

Let $Z_i[n] = |h_i[n]|^2 P_{i,e}^{UL}[n] + I_i[n]$

At SCA iteration i, the first-order Taylor expansion of $log_2(Z_i[n])$ around the current point $Z_i^{(k)}[n]$ gives:

$$log_2(Z_i[n]) \le log_2\left(Z_i^{(k)}[n]\right) + \frac{1}{ln\,2}\frac{Z_i[n] - Z_i^{(k)}}{Z_i^{(k)}} \quad (42)$$

Substituting (42) into (41) yields the following concave lower bound:

$$R_{i,b}[n] \ge Blog_2\left(|h_i[n]|^2\left(P_{i,b}^{UL}[n] + P_{i,e}^{UL}[n]\right) + I_i[n]\right) - B\left[log_2\left(Z_i^{(k)}[n]\right) + \frac{1}{ln\,2}\frac{Z_i[n] - Z_i^{(k)}}{Z_i^{(k)}}\right] \quad (43)$$

$$\triangleq R_{i,b}^{\sim(k)}[n]$$

Since $R_{i,b}^{\sim(k)}[n]$ is concave in the optimization variables, the original nonconvex bl-rate constraint can be replaced by the convex surrogate constraint. The same procedure is applied to the enhancement-layer UL rate, the A2A forwarding rate, the DL OMA rate thereby yielding a sequence of convex subproblems that are solved iteratively within the AO framework.

$$R_{i,b}^{\sim(k)}[n] \ge R_{i,b}^{min}$$

F. *DL POWER OPTIMIZATION*

In the downlink, orthogonal multiple access (OMA) is adopted. The DL rate:

$$R_i^{DL}[n] = B_{DL}log_2\left(1 + \frac{P_{i,u(i)}^{DL}[n]|h_i[n]|^2}{N_0}\right)$$

is concave in $\boldsymbol{P_{i,u(i)}^{DL}[n]}$. Therefore, the DL power allocation subproblem is a convex program under per-UAV power constraints.

G. *TRAJECTORY OPTIMIZATION*

For fixed communication variables, the trajectory optimization is still nonconvex due to the inverse-distance channel model. Introducing auxiliary variables:

$$m_i[n] \ge \left|\left|q_{u(i)}[n] - W_i\right|\right|^2 + H^2$$

allows the channel gain to be expressed as:

$$|h_i[n]|^2 = \frac{\beta_0}{m_i[n]}$$

The convex function $\frac{\beta_0}{m_i[n]}$ is approximated using first-order linearization at the current trajectory, which yields a convex trajectory subproblem. To handle the nonconvex trajectory dependence, define the auxiliary variable:

 doi:10.20944/preprints202603.2442.v1

$$m_i[n] \geq \left|\left|q_{u(i)}[n] - W_i\right|\right|^2 + H^2,$$

such that

$$|h_i[n]|^2 = \frac{\beta_0}{m_i[n]}$$

The function $\frac{\beta_0}{m_i[n]}$ is convex in $m_i[n]$ for $m_i[n] > 0$. Using first-order approximation at the current iterate $m_i^{(k)}[n]$, we obtain:

$$\frac{\beta_0}{m_i[n]} \geq \frac{\beta_0}{m_i^{(k)}[n]} - \frac{\beta_0}{\left(m_i^{(k)}[n]\right)^2}\left(m_i[n] - m_i^{(k)}[n]\right) \quad (44)$$

Equation (44) provides an affine lower bound on the channel gain, which is then substituted into the rate expressions to yield a convex trajectory subproblem.

H. *FANET OFFLOADING DECISION*

After solving the relaxed problem, the FANET decision is updated by comparing the enhancement-layer execution latency:

$$\xi_i = \begin{cases} 1, & \Delta_{i,e}^{A2A} + \Delta_{i,e}^{MEC@v} < \Delta_{i,e}^{MEC@u} \\ 0, otherwise. \end{cases}$$

This rule ensures that cooperative execution is adopted only when it reduces the overall enhancement-layer latency.

I. *OVERALL ALGORITHM*

The overall solution procedure is summarized as follows:

Algorithm 1 AO-SCA Algorithm for Priority-Aware SPC–NOMA UAV-MEC

Input: System parameters, initial feasible solution

$$(q^{(0)}, P^{UL,(0)}, P^{DL,(0)}, f^{(0)}, \xi^{(0)}), tolerance\ \epsilon$$

Output: Optimized variables $(q^*, P^{UL,*}, P^{DL,*}, f^*, \xi^*)$

Initialize iteration index $r = 0$

repeat

until convergence

1) **UL power Update:**

Fix $(q^{(r)}, P^{DL(r)}, f^{(r)}, \xi^{(r)})$ and solve the UL power allocation subproblem using SCA.

2) **DL power Update:**

Fix $(q^{(r)}, P^{UL(r+1)}, f^{(r)}, \xi^{(r)})$ and solve the convex DL power allocation problem.

3) **CPU Allocation:**

Update CPU frequencies using the closed-form solution

$$f_{i,b}^{MEC} = F_u^{max} \sqrt{\left(w_i S_{i,b}^{UL}\right)} / \sum_{j \in I_u}^{I} \sqrt{\left(w_j S_{j,b}^{UL}\right)}$$

4) **Trajectory Update:**

Fix communication variables and update UAV trajectories using SCA with the linearized channel gain.

5) **FANET Decision Update:**

Update ξ_i by comparing local and cooperative enhancement-layer execution latency.

Update objective value $J^{(r+1)}$

$r \leftarrow r + 1$

$|J^{(r)} - J^{(r-1)}| \leq \epsilon$

Return optimized solution.

 doi:10.20944/preprints202603.2442.v1

The algorithm monotonically decreases the objective value at each iteration and converges to a stationary point of the relaxed problem.

Lemma 3 (Convergence of AO–SCA Algorithm). The proposed AO–SCA algorithm generates a non-increasing sequence of objective values and converges to a stationary point of the relaxed problem.

Proof. At each iteration, the SCA procedure constructs a convex surrogate problem whose objective is a tight upper bound of the original objective at the current point. Therefore, the solution of the convex subproblem does not increase the objective value. Since the objective function is bounded below by zero (latency cannot be negative), the sequence of objective values is monotonically decreasing and convergent. Finally, using the properties of SCA and block coordinate descent methods, the algorithm converges to a stationary point of the convexified problem.

5. Results and Discussion

This section describes the simulation results and evaluation of the proposed framework. To evaluate the performance of the proposed scheme, extensive simulations are performed in comparison to fourth baseline schemes, i.e., Non-Cooperative Multi-UAV SPC–NOMA (NC-SPC), Fixed-Trajectory Cooperative SPC–NOMA (FT-Coop), Single-Layer NOMA MEC (SL-NOMA), and Layered OMA MEC (L-OMA). The *"NC-SPC"*, this baseline quantifies the gain due to FANET-assisted EL execution, while in*"FT-Coop"*, isolates the effect of trajectory-aware optimization, also *"SL-NOMA"*, evaluates the gain brought by layered task prioritization, and *"L-OMA"*, shows the contribution of non-orthogonal layered transmission. In this context, important performance evaluation criteria are considered for comparison: End-2-End latency, task completion rate, spectral efficiency, and computation latency. To evaluate the performance of the proposed framework comprehensively, important factors are considered: the number of UAVs, the number of users, UAV trajectory length, and UAV CPU frequency. All the schemes are implemented with the same simulation environment to evaluate the performance comprehensively.

Table 2. Simulation system's parameters [40].

Parameter	Value	Unit	Description
UE	60	-	Number of users
UAV	6	-	Number of UAVs
H_{min}	50	m	UAV minimum altitude
H_{max}	100	m	UAV maximum altitude
$d_{hor.}$	49	m	Horizontal distance between user i and UAV u
$d_{ver.}$	12	m	Maximum vertical distance
$d_{u,v}$	50	m	Distance between UAVs
P_u^{max}	5	watt	Maximum transmit power of UAV
P_i^{UL}	1	watt	Maximum transmit power of user device
F_u^{max}	10-20	Giga cycles/s	CPU frequency of UAV processor
F_i^{max}	1.5	Giga cycles/s	CPU frequency of UE device processor
S_i^{UL}	1-3	MB	UL data size
B	20	MHz	G2A channel bandwidth
B_{A2A}	40	MHz	A2A channel bandwidth

 doi:10.20944/preprints202603.2442.v1

B_{DL}	10	MHz	A2G channel bandwidth
N_0	-100	dBm	Noise power

The Figure 3 illustrates the effect of the number of UAVs on the E2E latency for different schemes: NC-SPC, FT-Coop, SL-NOMA, and L-OMA. It is clear that the E2E latency decreases with increasing UAVs numbers across all schemes, but it drops sharply when the number increases from 1 to 6, and then continues to decrease gradually.

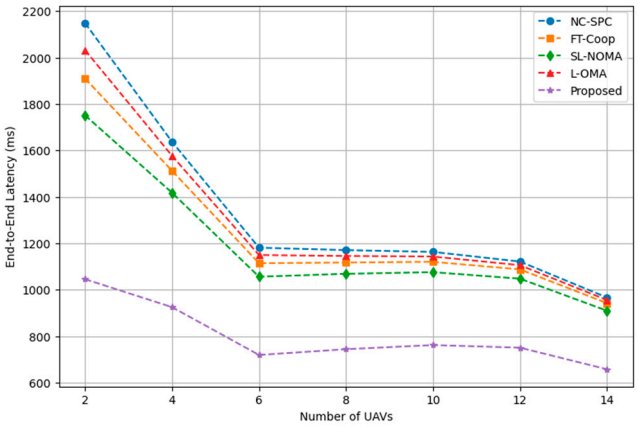

Figure 3. E2E latency versus number of UAVs for the proposed and baseline schemes.

It is also evident that the proposed scheme exhibits the lowest E2E latency across all UAV numbers, ranging from 1045.33 (ms) to 657.19 (ms), compared to the performance of the other schemes (see **Table 3**).

Table 3. Numerical results of E2E latency versus number of UAVs for the proposed and baseline schemes.

Number of UAVs	NC-SPC (ms)	FT-Coop (ms)	SL-NOMA (ms)	L-OMA (ms)	Proposed (ms)
2	2149.03	1910.05	1751.51	2032.34	1045.33
4	1637.39	1512.53	1417.93	1577.03	924.88
6	1181.09	1114.02	1055.88	1149.35	718.81
8	1170.61	1117.08	1068.54	1145.35	743.55
10	1162.74	1120.22	1075.53	1142.95	761.46
12	1121.30	1087.44	1047.49	1105.69	750.17
14	966.47	942.08	909.40	955.53	657.19

Figure 4 illustrates the behavior of E2E latency (ms) as a function of number of users across various schemes. it is clear from the figure that, as the number of users increases from 20 to 120, the end-to-end latency increases across all schemes.

 doi:10.20944/preprints202603.2442.v1

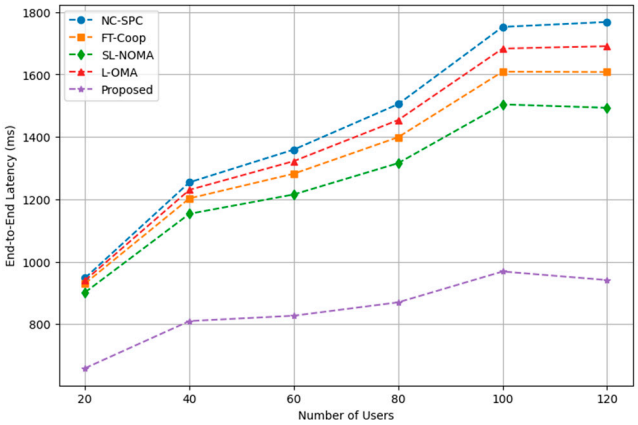

Figure 4. E2E latency versus number of users for the proposed and baseline schemes.

It is obviously NC-SPC exhibits the maximum E2E latency, followed by L-OMA and FT-Coop, while SL-NOMA has better performance. The proposed scheme has better performance compared to all schemes with significantly low E2E latency (658.83 ms to 941.25 ms) at all user densities.

Thus, it is clear that the proposed scheme is more robust in terms of handling a large number of users (scalability) with low E2E latency (see **Table 4**).

Table 4. Numerical results of E2E latency versus number of users for the proposed and baseline schemes.

Number of Users	NC-SPC (ms)	FT-Coop (ms)	SL-NOMA (ms)	L-OMA (ms)	Proposed (ms)
20	947.87	930.19	901.65	940.09	658.83
40	1254.43	1202.95	1153.50	1230.28	809.88
60	1359.30	1281.97	1215.61	1322.32	827.00
80	1504.92	1398.99	1315.84	1453.98	869.83
100	1752.40	1608.98	1504.13	1683.03	968.67
120	1768.19	1607.82	1493.25	1690.63	941.25

Figure 5 demonstrates the effect of UAV trajectory length (m) on E2E latency (ms) for various schemes. It is observed that as the trajectory length varies from 25 m to 150 m, the E2E for all schemes increases significantly because of the increased distance between UAV and user.

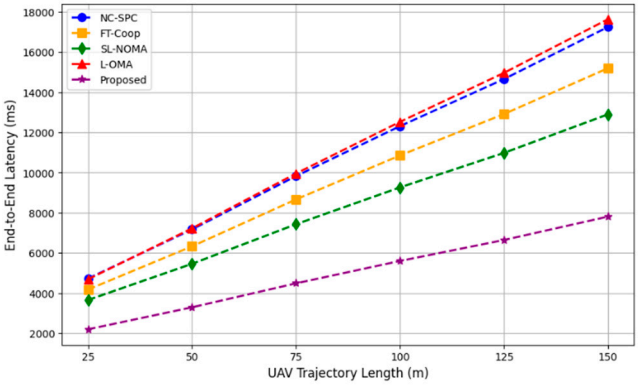

Figure 5. E2E latency versus UAV trajectory length for the proposed and baseline schemes.

Among all the baseline schemes, L-OMA and NC-SPC result in the highest latency, followed by FT-Coop, while SL-NOMA results in relatively lower latency. However, it is observed that the

 doi:10.20944/preprints202603.2442.v1

proposed scheme results in the minimum latency, i.e., in the range of 2203 ms to 7811 ms, for all trajectory lengths (see **Table 5**).

This demonstrates the efficiency of the proposed scheme in reducing the latency caused due to increased UAV trajectory length.

Table 5. Numerical results of E2E latency versus UAV trajectory length for the proposed and baseline schemes.

Trajectory Length (m)	NC-SPC (ms)	FT-Coop (ms)	SL-NOMA (ms)	L-OMA (ms)	Proposed (ms)
25	4728.95	4180.00	3662.05	4692.47	2203.5
50	7173.74	6332.16	5461.51	7225.88	3297.4
75	9825.67	8666.44	7430.86	9953.95	4490.7
100	12311.1	10853.4	9263.63	12525.7	5603.8
125	14653.8	12913.7	10980.5	14961.9	6647.3
150	17244.3	15194.2	12899.2	17632.3	7811.3

From the Figure 6, it can be observed that the computation latency decreases as the UAV CPU frequency increases from 5 GHz to 25 GHz for all the schemes, as the processing power of the CPU increases.

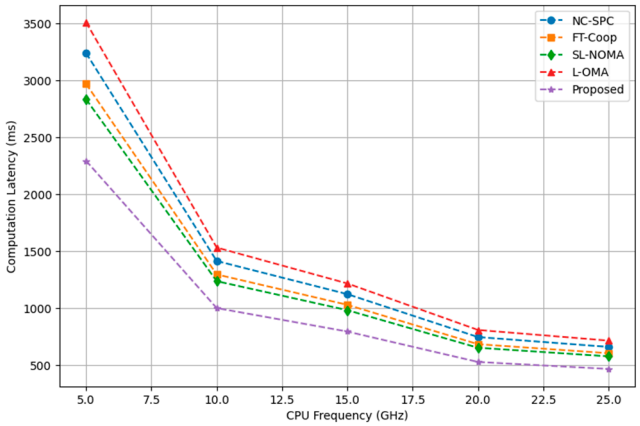

Figure 6. Computation latency versus UAV CPU frequency for the proposed and baseline schemes.

For the baseline schemes, the latency of the L-OMA scheme is the highest, followed by the NC-SPC and FT-Coop schemes, while the performance of the SL-NOMA scheme is relatively better than the others. However, the proposed scheme has the least latency, ranging from 2293.3 ms to 468.69 ms (see **Table 6**).

Table 6. Numerical results of computation latency versus UAV CPU frequency for the proposed and baseline schemes.

CPU Frequency (GHz)	NC-SPC (ms)	FT-Coop (ms)	SL-NOMA (ms)	L-OMA (ms)	Proposed (ms)
5.0	3237.65	2967.85	2832.94	3507.46	2293.3
10.0	1414.91	1297.00	1238.05	1532.82	1002.2
15.0	1124.28	1030.59	983.750	1217.97	796.36
20.0	747.96	685.63	654.469	810.29	529.80
25.0	661.68	606.54	578.970	716.82	468.69

 doi:10.20944/preprints202603.2442.v1

Figure 7 shows the spectral efficiency (bps/Hz) as a function of the number of users for various schemes, i.e., NC-SPC, FT-Coop, SL-NOMA, L-OMA, and the proposed AO-SCA scheme. As the number of users increases from 20 to 120, the spectral efficiency of all the schemes decreases (see **Table 7**), indicating the impact of increased interference in the network.

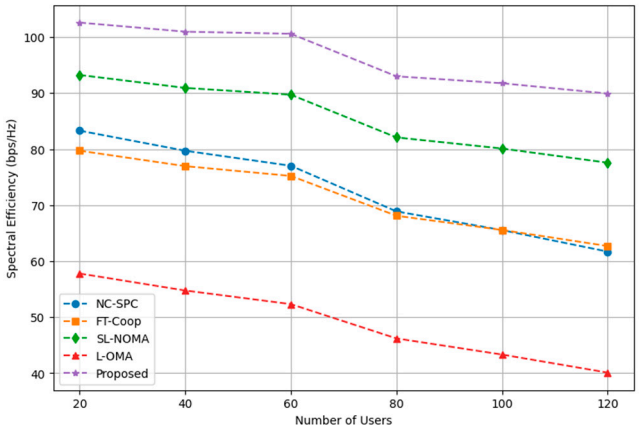

Figure 7. Spectral efficiency versus number of users for the proposed and baseline schemes.

Table 7. Numerical results of spectral efficiency versus number of users for the proposed and baseline schemes.

Number of Users	NC-SPC (bps/Hz)	FT-Coop (bps/Hz)	SL-NOMA (bps/Hz)	L-OMA (bps/Hz)	Proposed (bps/Hz)
20	83.2966	79.7205	93.2337	57.7961	102.58
40	79.7105	76.9651	90.9290	54.7641	100.96
60	77.0293	75.2150	89.7165	52.3346	100.59
80	68.8880	68.1090	82.0916	46.2124	92.998
100	65.5445	65.5721	80.1099	43.3322	91.762
120	61.7081	62.7008	77.5759	40.1102	89.917

It can be observed from (**Table 7**) that the proposed approach, i.e., AO-SCA, achieves the highest spectral efficiency for all the user densities, indicating the effectiveness of the proposed approach compared to NC-SPC, FT-Coop, SL-NOMA, and L-OMA schemes in terms of spectral efficiency.

Figure 8 illustrates the impact of number of users and number of UAVs on task completion rate. It is obviously when increasing the deployment of UAVs results in better performance for completing tasks, and performance deteriorates as user density increases. This shows resource limitations in dense scenario.

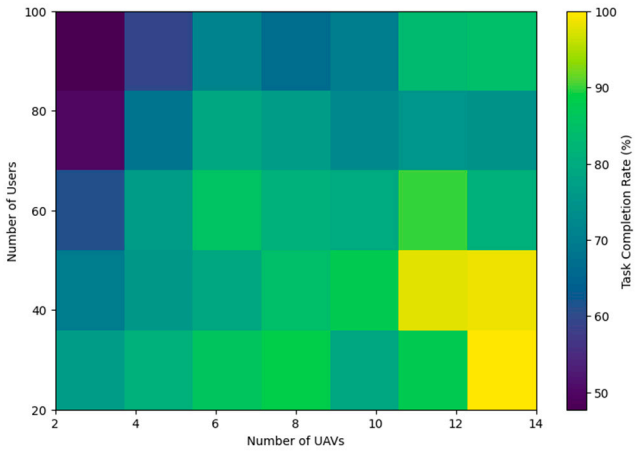

 doi:10.20944/preprints202603.2442.v1

Figure 8. Task completion rate versus number of UAVs and number of users for the proposed and baseline schemes.

Figure 9 presents the ratio of processed data to total generated data versus the number of users using different multiple access techniques such as NC-SPC, FT-Coop, SL-NOMA, L-OMA, and the proposed AO-SCA. It can be seen that when the number of users is set to 20, the efficiency of all the schemes is greater than 83%, with the proposed AO-SCA having the best performance at 92.3% (see **Table 8**). As the number of users increases to 120, the efficiency of all the schemes decreases due to network congestion and contentions. The efficiency of the NC-SPC scheme drops to 40.3%, the FT-Coop scheme drops to 51.3%, the SL-NOMA drops to 52.4%, the L-OMA drops to 45.3%, and the proposed AO-SCA still outperforms the other schemes with the best efficiency at 63.1%. This demonstrates the high data processing capacity of the proposed AO-SCA scheme, whereas the L-OMA scheme experiences the worst performance due to its orthogonal allocation limitation.

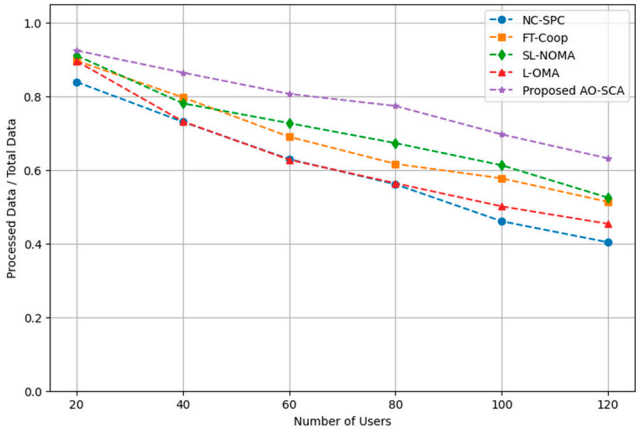

Figure 9. Processing efficiency vs number of users for the proposed and baseline schemes.

Table 8. Numerical results of processing efficiency vs number of users for the proposed and baseline schemes.

Number of Users	NC-SPC Ratio	FT-Coop Ratio	SL-NOMA Ratio	L-OMA Ratio	Proposed Ratio
20	0.838	0.896	0.910	0.895	0.923
40	0.730	0.796	0.780	0.731	0.863
60	0.629	0.689	0.726	0.627	0.806
80	0.561	0.616	0.672	0.563	0.773
100	0.460	0.576	0.612	0.500	0.696
120	0.403	0.513	0.524	0.453	0.631

Figure 10 illustrates the convergence performance of the proposed scheme in term of E2E latency with respect to the iteration count. As illustrated in the figure above, the E2E latency decreases rapidly from 416.46 ms at the first iteration to nearly 136.89 ms at the 20th iteration. After the 20th iteration, the E2E latency remains at nearly 120 ms. This demonstrates the performance of the proposed scheme as achieves steady-state performance with the least amount of fluctuations.

 doi:10.20944/preprints202603.2442.v1

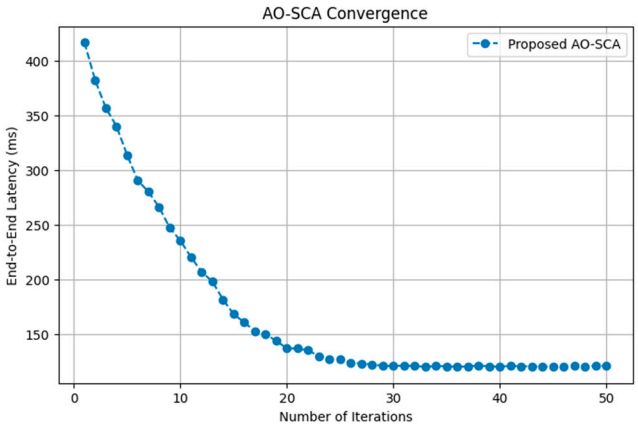

Figure 10. Objective convergence versus number of iterations for the proposed priority-aware AO-SCA algorithm.

It is clear from Figure 11 the proposed AO-SCA scheme always has the minimum latency for all thresholds. When the threshold is set to 600 ms, the latency of AO-SCA is less than that of NC-SPC, FT-Coop, SL-NOMA, and L-OMA, with reductions in latency of 39.2%, 35.5%, 32.1%, and 37.5%, respectively.

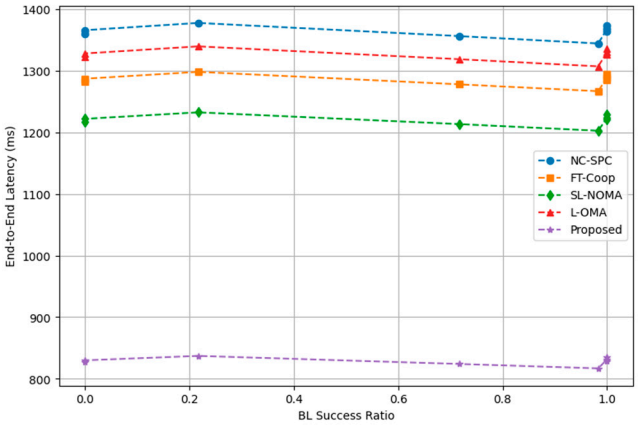

Figure 11. E2E latency versus BL success ratio for the proposed and baseline schemes.

The priority-aware design keeps BL reliability high across all schemes, however, the considerable latency differences of the proposed scheme prove its efficiency gains.

The Figure 12 depicts the effect of user density on BL latency. As the number of users varies from 20 to 120, it is observed that the latency for each scheme increases. The NC-SPC, FT-Coop, SL-NOMA, and L-OMA schemes show increased latency, ranging from 238.52 to 296.74 ms, 238.91 to 288.09 ms, 231.98 to 270.68 ms, and 240.42 to 308.15 ms, respectively.

 doi:10.20944/preprints202603.2442.v1

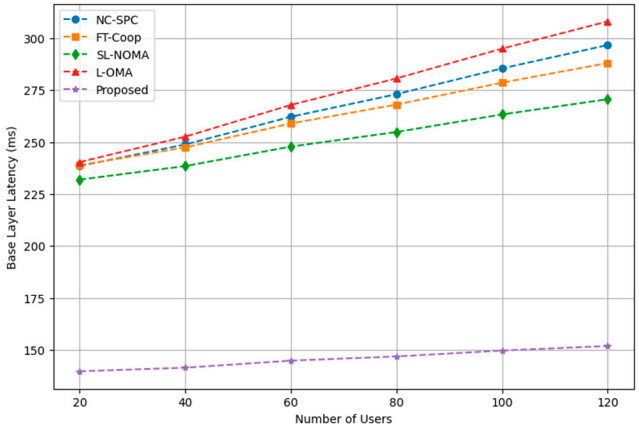

Figure 12. Base layer latency versus number of users for the proposed and baseline schemes.

On the other hand, it is also observed that the proposed AO-SCA scheme maintains the lowest latency for each value of user density, and its latency increases moderately from 139.68 ms to 151.87 ms.

It is noticed from Figure 13. that baselines schemes shows a high utilization even at low load regions which indicates overuse FANET cooperation and lack of intelligent cooperative processing decision (see **Table 9**). The latter is deployed efficiently by the proposed scheme which justifies that $\boldsymbol{\xi_i \sim 0}$ at low load, i.e. local processing is sufficient.

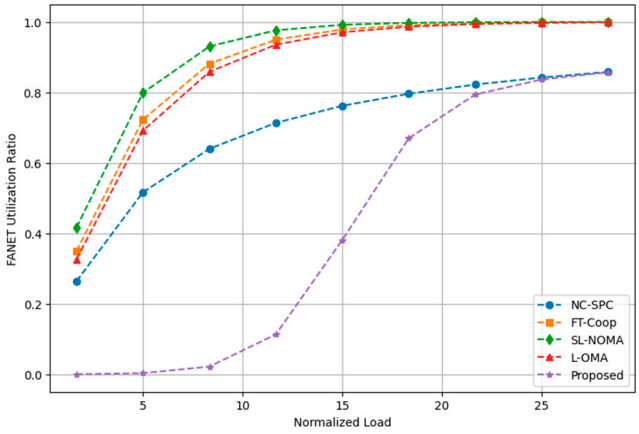

Figure 13. FANET utilization ratio versus normalized load for the proposed and baseline schemes.

Table 9. Numerical results of FANET utilization ratio versus normalized load for the proposed and baseline schemes.

Normalized Loaed	NC-SPC FANET Ratio	FT-Coop FANET Ratio	SL-NOMA FANET Ratio	L-OMA FANET Ratio	Proposed FANET Ratio
1.666	0.264	0.350	0.416	0.326	0.0
5.0	0.516	0.722	0.798	0.691	0.003
8.333	0.639	0.881	0.930	0.858	0.022
11.666	0.713	0.949	0.976	0.935	0.11
15.0	0.762	0.978	0.991	0.970	0.381
18.333	0.796	0.990	0.997	0.986	0.669
21.666	0.822	0.996	0.999	0.993	0.793
25.0	0.842	0.998	0.999	0.997	0.836
28.333	0.858	0.999	0.999	0.998	0.856

 doi:10.20944/preprints202603.2442.v1

6. Conclusions

The paper introduced a cooperative UAVs trajectory-aware SPC-NOMA layered transmission framework in mission-critical post-disaster scenario. In the proposed framework, the joint optimization of UAVs' trajectories, power allocation, and user association is carried out. This effectively increases the spectral efficiency and minimizes the overall latency in mission-critical communications. Moreover, the use of layered transmission in the proposed framework prioritizes the transmission of critical tasks. Simulation results have been provided, which prove that the proposed framework achieves fast convergence, low latency, and high efficiency in processing tasks compared to traditional baseline schemes. These results emphasize the significance of optimizing the trajectory of UAVs in UAV networks, as it directly influences the overall communication.

In future work, the adaptive optimization of UAVs' trajectories using AI and energy optimization in FANETs can be addressed.

Abbreviations

Symbol	Description
$S_{i,b}^{UL}$	Number of bits during BL
$S_{i,e}^{UL}$	Number of bits during EL
$P_{i,b}^{UL}$	Power allocated for BL
$P_{i,e}^{UL}$	Power allocated for EL
B	Transmission bandwidth
$S_{i,e}^{DL}$	Number of downloading bits
$P_{i,u}^{DL}$	Downlink transmit power allocated by UAV u to user i
$f_{i,b}^{MEC}$	A fraction of CPU frequency allocated to the $i-th$ users with constraints (unitless) to execute the BL task
$f_{i,e}^{MEC}$	A fraction of CPU frequency allocated to the $i-th$ users with constraints (unitless) to execute the EL task
N_0	Noise power

References

1. S. Jeong, O. Simeone, and J. Kang, "Mobile Edge Computing via a UAV-Mounted Cloudlet: Optimization of Bit Allocation and Path Planning," *IEEE Trans. Veh. Technol.*, vol. 67, no. 3, pp. 2049–2063, 2018, doi: 10.1109/TVT.2017.2706308.
2. G. Sun *et al.*, "Multi-objective Optimization for Multi-UAV-assisted Mobile Edge Computing," pp. 1–16.
3. A. R. Desher and A. Al-shuwaili, "Reliable Layered Transmission and Task Offloading in UAV-Assisted MEC Networks for Disaster Relief," pp. 1–20, 2026.
4. D. Kim, S. Member, J. Lee, and S. Member, "Joint Mission Assignment and Topology Management in the Mission-Critical FANET," *IEEE Internet Things J.*, vol. PP, no. c, p. 1, 2019, doi: 10.1109/JIOT.2019.2958130.
5. F. Banaeizadeh *et al.*, "Optimal UAV-trajectory design in a dynamic environment using NOMA and deep reinforcement learning To cite this version : HAL Id : hal-04762084 Optimal UAV-Trajectory Design in a Dynamic Environment Using NOMA and Deep Reinforcement Learning," 2024.
6. H. S. Ghazi, A. Al-shuwaili, A. R. Azeez, and M. Krasicki, "HYBRID NOMA-BASED RESOURCE ALLOCATION FOR MULTI-ACCESS EDGE COMPUTING IN HETNETS," pp. 38–51, 2025.
7. Z. Ding, J. Xu, O. A. Dobre, and H. V. Poor, "Joint Power and Time Allocation for NOMA-MEC Offloading," pp. 1–4.
8. P. Zhang *et al.*, "Deep Reinforcement Learning Based Computation Offloading in UAV-Assisted Edge Computing," *Drones*, vol. 7, no. 3, pp. 1–14, 2023, doi: 10.3390/drones7030213.
9. H. Li, Z. Jia, S. He, K. Guo, and Q. Wu, "Hierarchical Task Offloading for UAV-Assisted Vehicular Edge Computing via Deep Reinforcement Learning," vol. 001, no. 2024, 2025, [Online]. Available: http://arxiv.org/abs/2507.05722
10. W. Mao, K. Xiong, Y. Lu, and A. Background, "Energy Consumption Minimization in Secure Multi-antenna UAV-assisted MEC Networks with Channel Uncertainty," pp. 1–14.

 doi:10.20944/preprints202603.2442.v1

11. F. Zhou, Y. Wu, H. Sun, and Z. Chu, "UAV-Enabled Mobile Edge Computing : Offloading Optimization and Trajectory Design".
12. T. Zhang, Y. Xu, J. Loo, D. Yang, and L. Xiao, "Joint Computation and Communication Design for UAV-Assisted Mobile Edge Computing in IoT".
13. M. Li *et al.*, "Energy-Efficient UAV-Assisted Mobile Edge Computing : Resource Allocation and Trajectory Optimization," pp. 1–33.
14. L. Wang *et al.*, "RL-Based User Association and Resource Allocation for Multi-UAV enabled MEC".
15. X. Chen, T. Chen, Z. Zhao, H. Zhang, M. Bennis, and Y. Ji, "Resource Awareness in Unmanned Aerial Vehicle-Assisted Mobile-Edge Computing Systems," pp. 1–7.
16. A. Al-shuwaili and A. Lawey, "Achieving Low-Latency Mobile Edge Computing by Uplink and Downlink Decoupled Access in HetNets".
17. A. Bujari, C. E. Palazzi, and D. Ronzani, "FANET Application Scenarios and Mobility Models," pp. 43–46, 2017.
18. A. Chriki, H. Touati, H. Snoussi, and F. Kamoun, "FANET : Communication , mobility models and security issues," *Comput. Networks*, vol. 163, p. 106877, 2019, doi: 10.1016/j.comnet.2019.106877.
19. J. J. Ruz, O. Arévalo, G. Pajares, and J. M. De Cruz, "UAV Trajectory Planning for Static and Dynamic Environments," 2004.
20. N. Fanet, M. A. Khan, I. M. Qureshi, and F. Khanzada, "A Hybrid Communication Scheme for Efficient and Low-Cost Deployment of Future Flying Ad-Hoc," 2019, doi: 10.3390/drones3010016.
21. M. Ma, "Distributed Offloading for Multi-UAV Swarms in MEC-Assisted 5G Heterogeneous Networks," 2023.
22. A. C. Review, "UAV-Enabled Mobile Edge-Computing for IoT Based on AI : A Comprehensive Review," 2021.
23. I. Engineering, M. Photonics, and I. Engineering, "Machine learning based altitude-dependent empirical LoS probability model for air-to-ground communications ∗ #," vol. 23, no. 9, pp. 1378–1389, 2022.
24. Y. Zhang *et al.*, "Machine Learning-Based Reliable Transmission for UAV Networks with Hybrid Multiple Access," vol. 18, no. 9, 2020.
25. R. Abdallah, J. Gaber, R. Kouta, C. Sarraf, and M. Wack, "Reliability of data transmission of UAVs," pp. 1–4.
26. L. A. Al-haddad *et al.*, "Reliability-oriented framework for UAV-based inspection missions in modern power and energy systems," pp. 1–18, 2026.
27. Y. Zeng and R. Zhang, "Energy-Efficient UAV Communication with Trajectory Optimization," pp. 1–30.
28. T. M. Hoang, L. T. Dung, B. C. Nguyen, and T. Kim, "Performance analysis and optimization of UAV-assisted NOMA short packet," *ICT Express*, vol. 10, no. 2, pp. 292–298, 2024, doi: 10.1016/j.icte.2023.08.001.
29. U. A. V Networks, "Delay Minimization for BAC-NOMA Offloading in," pp. 1–16, 2025.
30. R. Han, Y. Wang, and Y. Zhang, "UAV - assisted NOMA secure communications : joint transmit power and trajectory optimization," *EURASIP J. Adv. Signal Process.*, vol. 5, 2023, doi: 10.1186/s13634-023-01056-5.
31. U. M. E. C. Systems, S. Wang, and Z. Luo, "An Energy-Efficient Scheme Design for NOMA-Based," pp. 1–15, 2024.
32. Y. Ai, C. Liu, and M. Li, "Energy-Efficient Uplink Communication in UAV-Enabled MEC Networks with Pinching Antennas," 2025.
33. T. Offloading, Q. Wu, M. Cui, G. Zhang, B. Zheng, and S. Member, "Energy-Efficient UAV-Enabled MEC Systems :," pp. 1–16.
34. M. T. Mamaghani, X. Zhou, N. Yang, and A. L. Swindlehurst, "Secure Short-Packet Transmission with Aerial Relaying : Blocklength and Trajectory Co-Design," 2023.
35. J. Lei, T. Zhang, S. Member, and X. Mu, "NOMA for STAR-RIS Assisted UAV Networks," pp. 1–30.
36. L. Xiang, K. Xu, S. Member, J. Hu, S. Member, and C. Masouros, "Robust NOMA-assisted OTFS-ISAC Network Design with 3D Motion Prediction Topology," pp. 1–10.
37. A. Y. Sadeeq and M. A. Ahmed, "UAV-BS-based Hybrid OMA-NOMA System with Multiple Antennas for Multi-user Communication," 2025.

 doi:10.20944/preprints202603.2442.v1

38. Q. Liu, L. Shi, L. Sun, J. Li, M. Ding, and F. S. Shu, "Path Planning for UAV-Mounted Mobile Edge Computing with Deep Reinforcement Learning," *IEEE Trans. Veh. Technol.*, vol. 69, no. 5, pp. 5723–5728, 2020, doi: 10.1109/TVT.2020.2982508.
39. T. Report, "TR 138 901 - V18.0.0 - 5G; Study on channel model for frequencies from 0.5 to 100 GHz (3GPP TR 38.901 version 18.0.0 Release 18)," vol. 0, 2024.
40. H. Hao, C. Xu, W. Zhang, S. Yang, and G. Muntean, "Joint Task Offloading , Resource Allocation , and Trajectory Design for Multi-UAV Cooperative Edge," *IEEE Trans. Mob. Comput.*, vol. 23, no. 9, pp. 8649–8663, 2024, doi: 10.1109/TMC.2024.3350078.

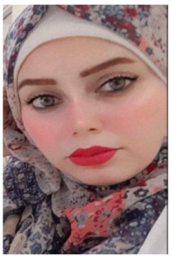

ANFAL R. DESHER received her B.Sc. degree in Mobile Communications and Computing Engineering from the University of Information Technology and Communications, Baghdad, Iraq in (2021) and is currently pursuing a Master of Engineering degree in the same field. She worked as a lecturer at the Faculty of Engineering, University of Information Technology and Communications for two years. Since May 2022, she is working as a lecturer at Uruk University in Baghdad, Iraq. Her research focuses on wireless communication networks, UAV communications, mobile edge computing, and intelligent intrusion detection systems for secure communications.

ALI NAJDI AL-SHUWAILI gained a Ph.D. degree in electrical engineering from New Jersey Institute of Technology (NJIT), Newark 07012, NJ, USA. Before that, he received the M.Sc. and B.Sc. degrees in communication engineering from Electrical and Electronic Engineering (EEE) department at University of Technology, Baghdad, Iraq. Currently he holds "dean assistant dean for scientific affairs" position at College of Engineering, UOITC. His research interests are in wireless communications, information theory, optimization and machine learning.